ARCHITECTURAL RESEARCH, Vol. 20, No. 2(June 2018). pp. 53-64 pISSN 1229-6163 eISSN 2383-5575

Analytical Modeling for Two-story Two-span Reinforced Concrete Frames with Relaxed Section Details

Taewan Kim, Yurim Chu and Hong-Gun Park

Department of Architectural Engineering, Kangwon National University, Chuncheon, South Korea
Department of Architectural Engineering, Kangwon National University, Chuncheon, South Korea
Department of Architecture and Architectural Engineering, Seoul National University, Seoul, South Korea

https://doi.org/10.5659/AIKAR.2018.20.2.53

Abstract A nonlinear analytical model has been proposed for two-span two-story reinforced concrete frames with relaxed section details. The analytical model is composed of beam, column, and beam-column joint elements. The goal of this study is to develop a simple and light nonlinear model for two-dimensional reinforced concrete frames since research in earthquake engineering is usually involved in a large number of nonlinear dynamic analyses. Therefore, all the nonlinear behaviors are modeled to be concentrated on flexural plastic hinges at the end of beams and columns, and the center of beam-column joints. The envelope curve and hysteretic rule of the nonlinear model for each element are determined based on experimental results, not theoretical approach. The simple and light proposed model can simulate the experimental results well enough for nonlinear analyses in earthquake engineering. Consequently, the proposed model will make it easy to developing a nonlinear model of the entire frame and help to save time to operate nonlinear analyses.

Keywords: Analytical Model, Reinforced Concrete Frame, Beam-column Joint, Cyclic Behavior, Relaxed Detail, Earthquake Engineering

1. INTRODUCTION

In reinforced concrete (RC) structures, most studies have usually aimed at developing special details that possess high ductility to be able to resist large lateral deformation. However, a demand for moderate details still exists in the low-to-mid seismic zone like Korea since many engineers insist the special details may be excessive and construction workers raise difficulties. Considering the demand, reinforced concrete (RC) columns with relaxed but comparable to special details have been tested at Structural Performance Enhancement Research Center (SPEC), which are summarized in journal papers (Kim et al., 2015a; Kim et al., 2015b; Kim et al., 2016a). The relaxed details include 90° hook stirrups and wider stirrup spacing than code-specified one. The experimental studies must become more valuable when their results can be the basis of analytical models whose appropriateness is very significant for the reliability of analytical studies that are necessary for earthquake engineering. An analytical model for the columns with relaxed details has been already proposed in Kim et al. (2017). The study aimed at proposing a simple nonlinear model to be able to simulate the hysteretic behavior of the relaxed details based on the results from the experimental studies.

Besides the column testing, beam-column joints with relaxed details, which include wider stirrup spacing inside the joint and shorter development length than code specified ones, are tested and the result is summarized in Kim et al. (2016a). Analytical modeling of the beam-column joints with relaxed details is one of the goals of this study. Finally, two-story two-span frames have been tested by applying the columns and beam-column joints with the relaxed details (Park, 2017). Three frames are selected; one of them is an intermediate moment frame for comparing with the other two alternative frames with relaxed detail. Analytical modeling of the two-story two-span frames with relaxed details is another goal of this study.

This article is just the sequel one of the previous one (Kim

Corresponding Author: Yurim Chu
Department of Architectural Engineering,
Kangwon National University, Chuncheon, South Korea
e-mail: yurim92@kangwon.ac.kr

This research was supported by a grant (13AUDP-B066083-01) from Architecture & Urban Development Research Program funded by Ministry of Land, Infrastructure and Transport of Korean government.

et al., 2017) covering analytical modeling of the columns with relaxed details. Therefore, modeling issues for column (or beam) members can be referred to the previous article. This study focuses on analytical modeling of beam-column joints with relaxed details (specially shear modeling of a joint region), and analytical modeling of two-story two-span frames consisting of beams, columns, and beam-column joints with the relaxed details. It is noted that approach to the goals in this study is identical to the previous article (Kim et al., 2017). The approach is to use lumped hinge models where the nonlinear hysteretic behaviors are concentrated on both ends of each member and to set the hysteretic behaviors to be consistent with experimental results.

2. ANALYTICAL MODEL FOR REINFORCED CONCRETE BEAM-COLUMN JOINTS

2.1. Analytical models for reinforced concrete beam and column members

A reinforced concrete beam-column joint is composed of a beam(s), a column(s), and a joint region. Therefore, element models for beams and columns should be defined along with that for a joint region in order to complete an analytical model for a beam-column joint. In the previous study (Kim et al., 2017), an element model for columns has been only proposed, which consists of an elastic element for the entire column length and a zero-length element at the end of the column. Nonlinear flexural behavior is concentrated on the zero-length element, which is represented by moment-rotation relationship. This approach can be directly applied to the element model for beam members because concentration of nonlinear behavior on lumped plastic hinges at the ends of beams or columns is identical. The detailed approach is not described herein but can be found in Kim et al. (2017).

2.2. Analytical models for reinforced concrete beam-column joints

There are various ways to model RC beam-column joints but *Joint2D* element provided by OpenSees (OpenSees, 2006) is only introduced herein. OpenSees provides another element for beam-column joints, *BeamColumnJoint* element (Altoonatash, 2004). The *BeamColumnJoint* element may simulate sliding of re-bars, shear at the contact surface between a joint and columns (or/and beams), and shear at the joint region. This element has a benefit to be able to simulate various behaviors of beam-column joints but too many input variables may decrease usefulness. On the other hand, the *Joint2D* element models shear behavior at the joint region and flexural behavior at the contact surface between the joint and columns (or/and beams) as rotational springs (refer to Figure 1). The shear behavior of the joint region is represented by a rotational spring in the *Joint2D* element. Furthermore, the entire behavior at the contact surface including shear and sliding of re-bars is represented by a rotational spring, which means that the entire behavior at the surface is represented by the moment-rotation relationship in the *Joint2D* element. The moment-rotation relationship rather than the moment-curvature relationship is convenient to make input models, conduct dynamic analyses, and check analysis results, which has already mentioned in the previous study (Kim et al., 2017). Consequently, the *Joint2D* element is utilized for analytical modeling of RC beam-column joints in this study. More detailed information for the modeling will be provided in later.

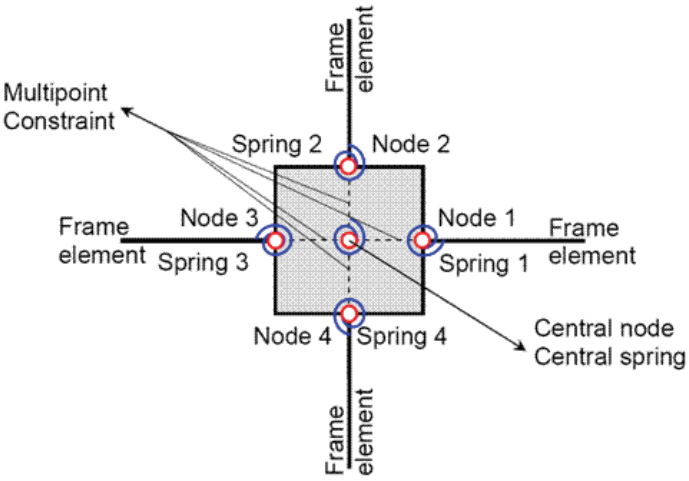

Figure 1. *Joint2D* element in OpenSees (Altoonatash, 2004)

3. SUMMARY OF LABORATORY TESTS

3.1. Beam-column joint tests

The experimental parameters for beam-column joint tests are a shape of joints, spacing of transverse reinforcement, and anchorage of longitudinal reinforcement of beams. The shapes are divided into external joint (T-type) and internal joint (cross-type). Table 1 presents the experimental parameters of test specimens. The test specimens consist of six external joints (EN, ER1, EU1, ER2, EU2, EU2C) and two internal joints (IN, IR). 'E' and 'I' denote external and internal joints, respectively. 'N', 'R', and 'U' denote details of transverse reinforcement inside the joint; 'N' denotes no transverse reinforcement, 'R' denotes transverse reinforcement with hoop and D10 cross tie, and 'U' denotes transverse reinforcement with U-stirrup. More detailed difference between specimens can be noticed in Table 1. The details of longitudinal and transverse reinforcement of beam-column joints are shown in Figure 2. Dimensions and reinforcement details of beam-column joint specimens are shown in Figure 3. Reinforcement details of columns are all same except for EU2C. For internal joints, IN and IR, the sum of the flexural strength of left and right beams are 1.45 times larger than that of upper and lower columns (weak column-strong beam). On the other hand, the flexural strength of column is a little larger than that of right beam.

Table 1. Parameters of beam-column joint specimens

Specimen	Type	Beams			Columns		Beam-column joints
		$b_b \times h_b$ (mm×mm)	Top bars	Bottom bars	$b_c \times h_c$ (mm×mm)	Longitudinal bars	Transverse reinforcement (ρ''*)
EN ER1 EU1	External	350×480	4D25 (1.21%)	2D25 (0.6%)	350×350	8D22 (2.53%)	N/A D13 hoops & D10 crossties @160mm (0.29%) D13 hoops & D10 crossties @160mm (0.29%)
ER2 EU2	External	350×480	7D19 (1.20%)	4D19 (0.68%)	350×350	8D22 (2.53%)	D13 hoops & D10 crossties @100mm (0.58%) D13 hoops & D10 crossties @100mm (0.58%)
EU2C	External	350×480	7D19 (1.20%)	4D19 (0.68%)	350×450	4D22+4D25 (2.27%)	D13 hoops & D10 crossties @100mm (0.63%)
IN IR	Internal	350×480	7D19 (1.20%)	4D19 (0.68%)	350×350	8D22 (2.53%)	N/A D13 hoops & D10 crossties @100mm (0.73%)

* ρ'' = volumetric ratio of horizontal confinement reinforcement in the joint

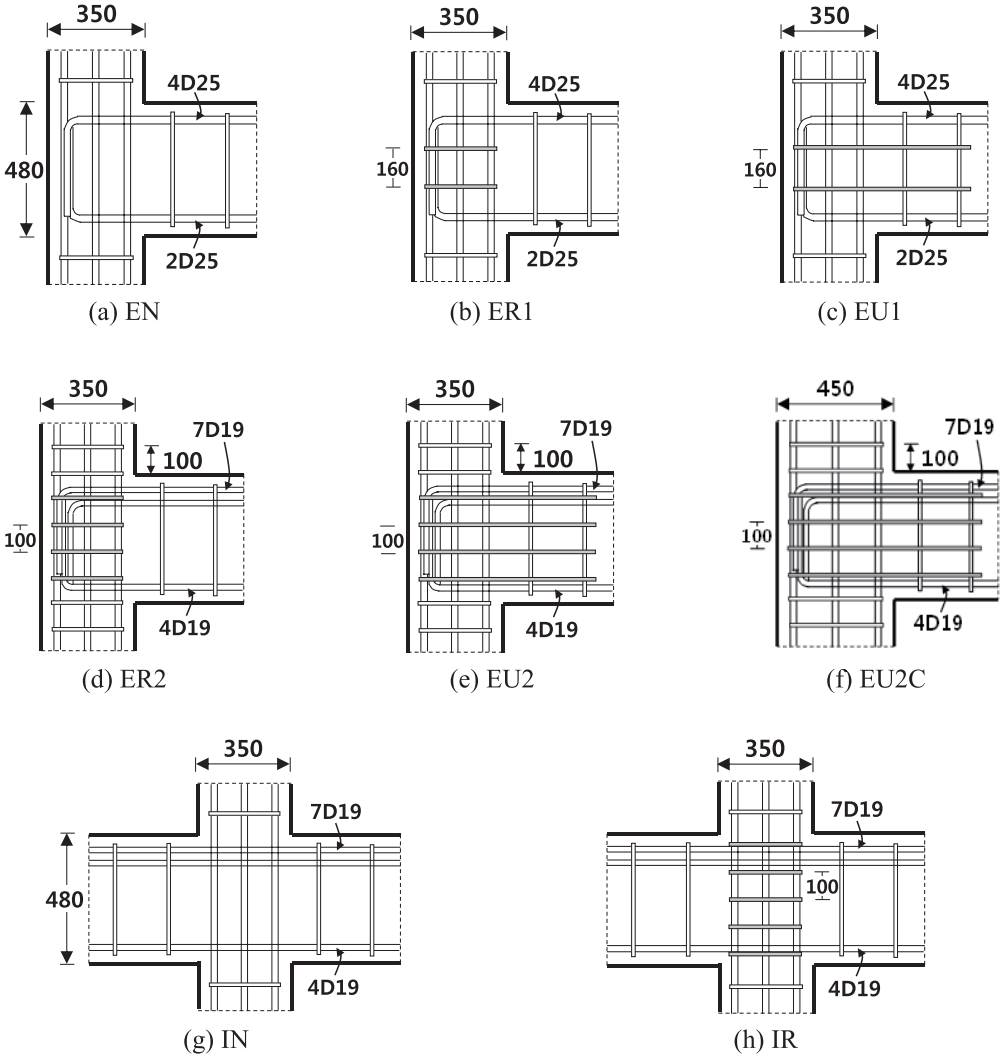

Figure 2. Details of longitudinal and transverse reinforcement of beam-column joints

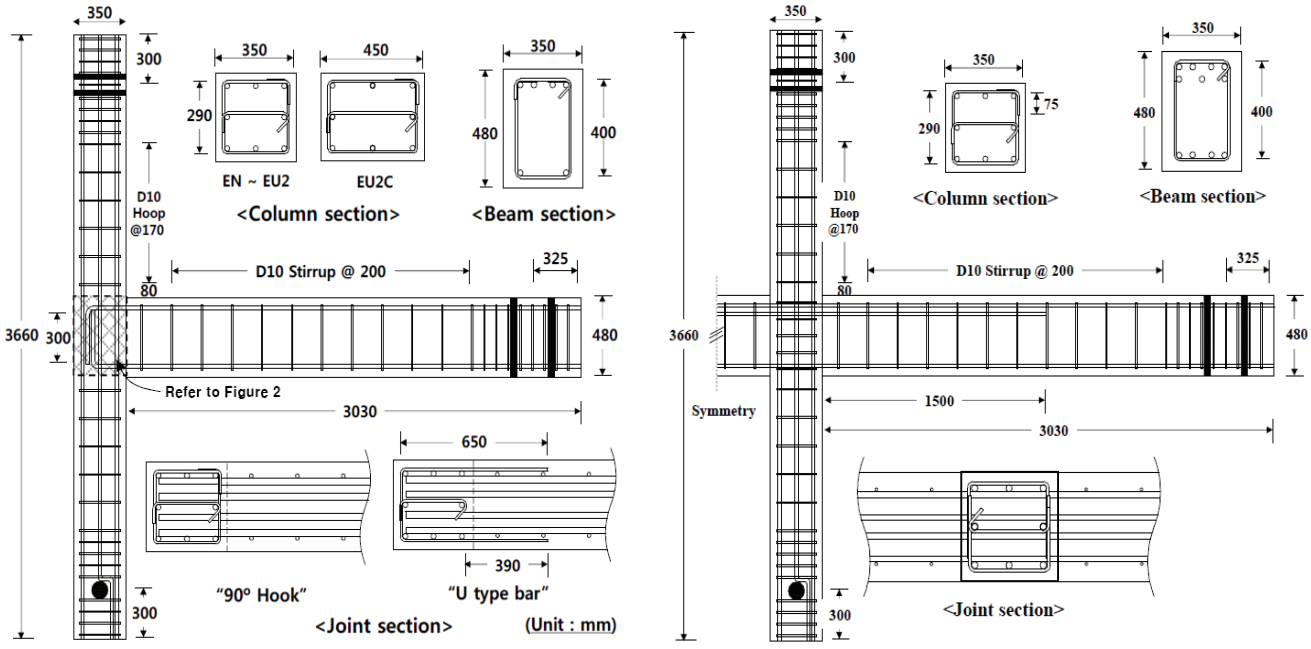

(a) External beam-column joint (b) Internal beam-column joint

Figure 3. Dimensions and reinforcement details of beam-column joint specimens (Kim et al., 2016a)

3.2. Two-story two-span frame tests

Three two-story two-span frame specimens are; intermediate moment frame (IMF), alternative 1 frame (A1F), and alternative 2 frame (A2F), where reinforcement detail is a main experimental parameter. IMF has seismic reinforcement details designed per current Korean Building Code (KBC) (2016). A1F has an identical strength to IMF, but stirrup details are a little relaxed, which includes 90° hook and stirrup spacing of $0.5H_{min}$ (minimum dimension) and 0.5d (effective depth) for beams and columns respectively. A2F is based on A1F except that longitudinal reinforcement ratios of beams and columns are increased by 40% from those in A1F. This is aimed for identifying the performance of the alternative frames by increasing shear demand inside beam-column joints. Detailed information for each specimen is presented in Table 2.

The stirrup details of columns in IMF and A1F (and A2F) adopt those of SAd2 and SBd2, respectively, which are presented in detail in Kim et al. (2015a). The stirrup details of beam-column joints in IMF adopt ER2 and IR for external and internal joints, respectively. The stirrup details of external beam-column joints in A1F (and A2F) adopt EU1 and EU2 in the second and the first story, respectively. The stirrup details of internal beam-column joints in A1F (and A2F) adopt EN and IN in the second and the first story, respectively. The stirrup details in A1F and

Table 2. Information for two-story two-span frame specimens

			IMF	A1F	A2F
Beam	Size (mm)		280 × 320	280 × 320	280 × 320
	Top	Re-bar	8-D13	8-D13	10-D13
		Ratio (%)	1.13	1.13	1.42
	Bottom	Re-bar	4-D13	4-D13	6-D13
		Ratio (%)	0.57	0.57	0.85
	d (mm)		260	260	260
	s (mm)	End	65	130	130
		Middle	130	130	130
Column	Size (mm)		280 × 280	280 × 280	280 × 280
	R-bar		6-D16	6-D16	6-D19
	Reinf. Ratio		1.52	1.52	2.19
	d (mm)		240	240	240
	s (mm)		140	140	140
Joint	Type		Internal/External	External	External
	Stirrup detail		135° hook	U-bar	U-bar
	s (mm)		70	70	70

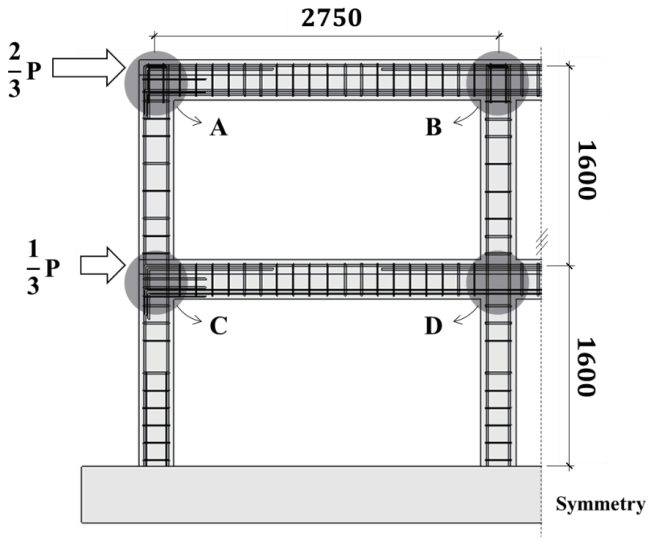

Figure 4. Test set up of two-story two-span frame specimens

A2F are identical to each other, but the amount of longitudinal re-bars is different as presented in Table 2. The arrangement of stirrup details for frames is summarized in Table 3. The alphabets (A, B, C, and D) indicate the location of beam-column joints, which are shown in the test set up of frame specimens (Figure 4).

Table 3. The arrangement of stirrup details for Two-story Two-span Frames

Specimen	Beam-Column Joint				Column
	A	B	C	D	
IMF	ER2	ER2	ER2	IR	SAd2
A1F	EU1	EN	EU2	IN	SBd2
A2F	EU1	EN	EU2	IN	SBd2

The central column in the first story of specimen IMF yields at story drift of 0.75% ~ 1.0%. The base shear of IMF reaches its maximum (346.8 kN, -336.7 kN) at story drift of 2.5%, and then drops below 80% of the maximum at story drift of 3.5%. This IMF specimen has 135° hook stirrups and smaller stirrup spacing than the other specimens, so it shows large deformation capability. In case of specimen A1F that has the same strength as IMF but relaxed stirrup details, the central column in the first story yields at story drift of 0.75%. The base shear of A1F reaches its maximum (367.0 kN, -346.4 kN) at story drift of 2.0%, and then drops below 80% of the maximum at drift ratio of 3.5%. It can be noticed that strength of IMF and A1F is similar, but deformation capability of A1F is lower than that of IMF since A1F has 90° hook and U-bar stirrups. A2F is tested for verification of A1F by means of increasing shear

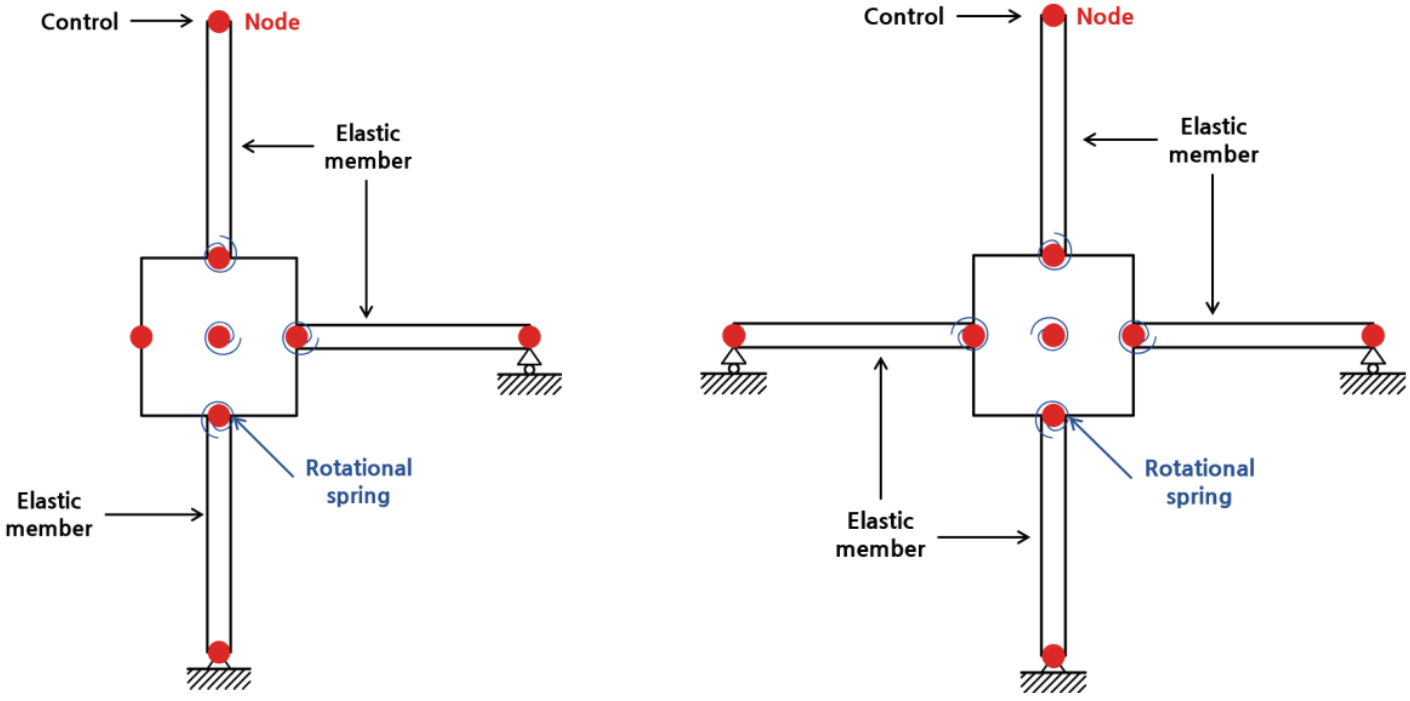

(a) External joint (b) Internal joint

Figure 5. Schematic drawings of beam-column joint model for rest specimens

demand of columns and beam-column joints. The central column in the first story of specimen A2F yields at story drift of 0.75% ~ 1.0%. The base shear of A2F reaches its maximum (390.1 kN, -362.2 kN) at story drift of 1.5%, and then drops below 80% of the maximum at drift ratio of 2.0%. As the result, increasing longitudinal re-bars and using relaxed details may have a negative effect on deformation capability. More detailed results are presented in Park (2017).

4. COMPARISON OF CYCLIC BEHAVIORS OF BEAM-COLUMN JOINTS FROM ANALYTICAL MODELS AND EXPERIMENTS

4.1 Analytical modeling of beam-column joint test specimens

An analytical model of beam-column joint consists of beam(s), columns, and a joint. The *Joint2D* element for a joint is composed of five nodes defined as rotational spring. Four of them are used for slip of re-bars at contact surface between the joint and beams/columns, and one of them located at the center of the joint is used for shear behavior of the joint. The slip of re-bars is not directly reflected on the analytical model for easy and simple modeling in this study. It then, nonlinear material model does not have to be defined at those four nodes. However, flexural plastic hinges at columns ends modeled by *zeroLength* element in Kim et al. (2017) can be modeled in the four rotational springs in the *Joint2D* element because both are rotational springs defined by moment-rotation. Therefore, *Pinching4* material model inputted in the *zeroLength* element for column model can be assigned to the four rotational springs in the *Joint2D* element. For beam and column members, the entire length except these nodes is defined as an elastic member modeled by *elasticBeamColumn* element. Figure 5 shows schematic drawings of beam-column joint model for test specimens.

Shear behavior of beam-column joint is represented by a rotational spring located at the center of the joint. The rotational spring must be defined by moment-rotation, so shear at the joint must be transformed into a moment. The *Pinching4* material model is also used for the shear behavior of the joint. Figure 6 shows a general hysteretic shear behavior of RC beam-column joints. In order to simulate the hysteretic shear behavior of the joint, tri-linear envelope curve is used, and pinching,

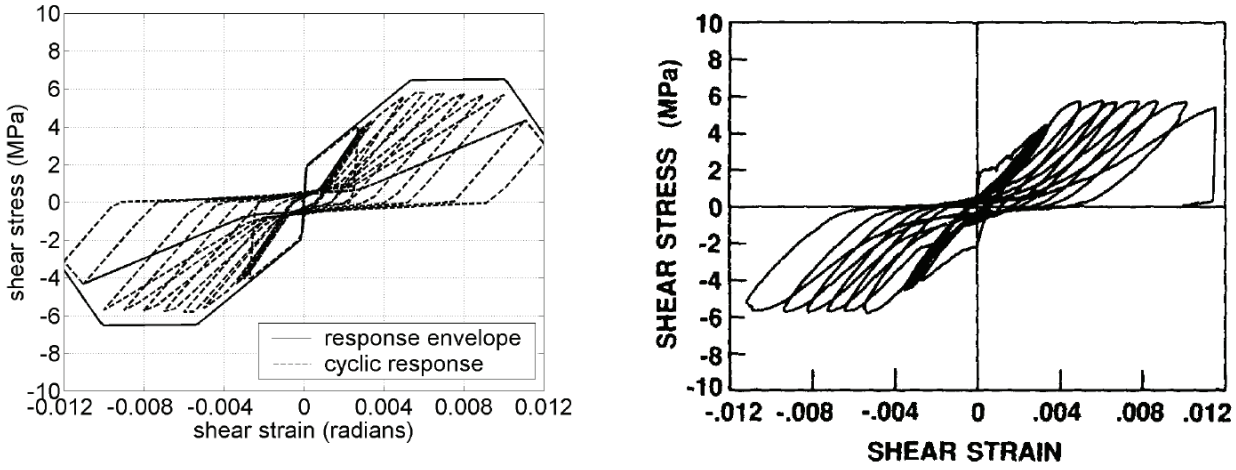

(a) Analysis (b) Experiment

Figure 6. Behavior of reinforce concrete panel, SE8 (Stevens et al [16])

Table 4. Values of *rDisp* and *fFoce* for *Pinching4* element

	Parameter	External Joint			Internal Joint	
		EN	ER1/EU1/ER2/EU2	EU2C	IN	IR
Positive	rDispP	0.3	0.2	0.4	0.2	0.3
	fFoceP	0.1	0.1	0.5	0.2	0.25
Negative	rDispN	0.2	0.2	0.3	0.2	0.2
	fFpceN	0.1	0.1	0.5	0.2	0.2

unloading stiffness deterioration, and accelerated reloading stiffness deterioration are utilized for hysteretic model. The strength at the envelope curve is estimated by general joint strength equations in KBC (2016). Deformation capacities are determined from test results.

The location where pinching initiates is defined by *rDisp* (the ratio of the deformation at which reloading occurs to the minimum historic deformation demand) and *rForce* (the ratio of the force at which reloading begins to force corresponding to the minimum historic deformation demand), which are adjusted depending on the shapes of hystereses. As can be seen in Figure 7 and Figure 8, the locations where pinching initiates and the areas enclosed by hysteretic curves especially in the second and fourth quadrants are different for the specimens. The determined values of *rDisp* and *fFoce* are presented in Table 4. Both variables for a specimen not reinforced by transverse reinforcement (EN) and the other reinforced specimens (EN, ER1, EU1, ER2, EU2) in external joints are almost identical except positive *rDisp* for EN. However, both variables for EU2C are larger than those for the other external joints, where a joint area of EU2C is larger than that of the other external joints. The area of the second and fourth quadrants in hysteretic curves for EU2C is also larger than that for the other external joint specimens. It can be noticed that the increase of joint area induces the increase of the area enclosed by hysteretic curves, that is to say, the increase of energy dissipation capacity. For internal joints, both variables are not much different, which implies lateral reinforcing in internal joints can affect deformation capacity, not pinching behavior much.

$$\delta_i=\alpha1\cdot\left(\tilde{d}_{max}\right)^{\alpha3}+\alpha2\cdot\left(\frac{E_i}{E_{monotonic}}\right)^{\alpha4} \quad (1)$$

$$\tilde{d}_{max}=\max\left[\frac{d_{max\,i}}{def_{max}},\frac{d_{min\,i}}{def_{min}}\right] \quad (2)$$

Unloading stiffness deterioration represents that stiffness gets decreased when a component is unloaded as compared to the previous cycle. Accelerated reloading stiffness deterioration represents that stiffness gets decreased when a component is reloaded. For unloading stiffness deterioration, the values of 1.3 and 0.2 are assigned for α1 and α3, respectively, which are the same values for columns presented in Kim et al. (2017). The α1 and α3 are variables inside a general form of the damage index by Park and Ang (1985).

The second part of equation (1) is to reflect an increase of energy dissipation, which is not considered in this study because it is too hard to control. Therefore, α2 and α4 in equation (1) are neglected in this study. In Equation (2), d_{max} and d_{min} are positive and negative maximum displacements at history, respectively. def_{max} and def_{min} are positive and negative displacements at failure, respectively. The parameter (δ_i) is the same as δk_i in Equation (3), which controls degradation ratio for unloading stiffness deterioration. In equation (3), k_o is initial stiffness before damage occurs, and k_i is current unloading stiffness.

$$k_i=k_o\cdot(1-\delta k_i) \quad (3)$$

In the previous study (Kim et al., 2017), unloading stiffness deterioration is only utilized for columns. The reason why accelerated reloading stiffness deterioration is utilized for beam-to-column joints is that hysteresis goes toward a location further than that in the previous cycle, which results in a decrease of stiffness when reloaded as can be noticed in Figure 7 and Figure 8. The way to simulate this reloading stiffness deterioration is similar to but different from that for unloading stiffness deterioration. Both deterioration modes utilize the damage index of equation (1), but the former decreases current stiffness indirectly by multiplying the maximum historic deformation demand by $(1+\delta d_i)$ as presented in equation (4) while the latter decreases current stiffness by multiplying the initial stiffness k_o by $(1-\delta k_i)$ as presented in equation (3).

$$d_{max\,i}=d_{max\,o}\cdot(1+\delta d_i) \quad (4)$$

where $d_{max\,i}$ is the deformation demand that defines the end of the reloading cycle for increasing deformation demand, $d_{max\,o}$ is the maximum historic deformation demand, and δd_i is the same as δ_i. In order to simulate this accelerated reloading stiffness deterioration, α1 is adjusted for each specimen while α3 is fixed to be 0.2 for all the specimens. As the result, α1 is assigned to be 0.3 for EN, 0.35 for ER1, 0.4 for EU1, ER2 and EU2, 0.2 for EU2C, 0.5 for IN, and 0.3 for IR.

4.2. Comparison of cyclic behaviors from analytical models and experiments

Cyclic behaviors of external and internal beam-column joints from analytical models and experiments are shown in Figure 7 and Figure 8, respectively. As can be noticed in the figures, the hysteretic curves from analyses simulate those from experiments pretty well. However, as in the case of columns, stiffness and strength degradation when cyclic loads are repeated at the same displacement and after strength reaches its maximum is not completely simulated (Kim et al., 2017). As described in the study, it can be achieved by representing basic strength deterioration and post-capping strength deterioration by adjusting both parts of the damage index (refer to equation (1)) properly, which would be very time consuming and would output results to be feasible for the case only. Considering this situation, this study makes an effort to simulate basic features of hysteretic curves such as unloading stiffness deterioration, accelerated reloading stiffness deterioration, and post-capping strength decrease by adjusting envelope curves and displacement part of the damage index. Consequently, Figure 7 and Figure 8 show that the proposed analytical model for beam-column joints can simulate experimental results satisfactorily.

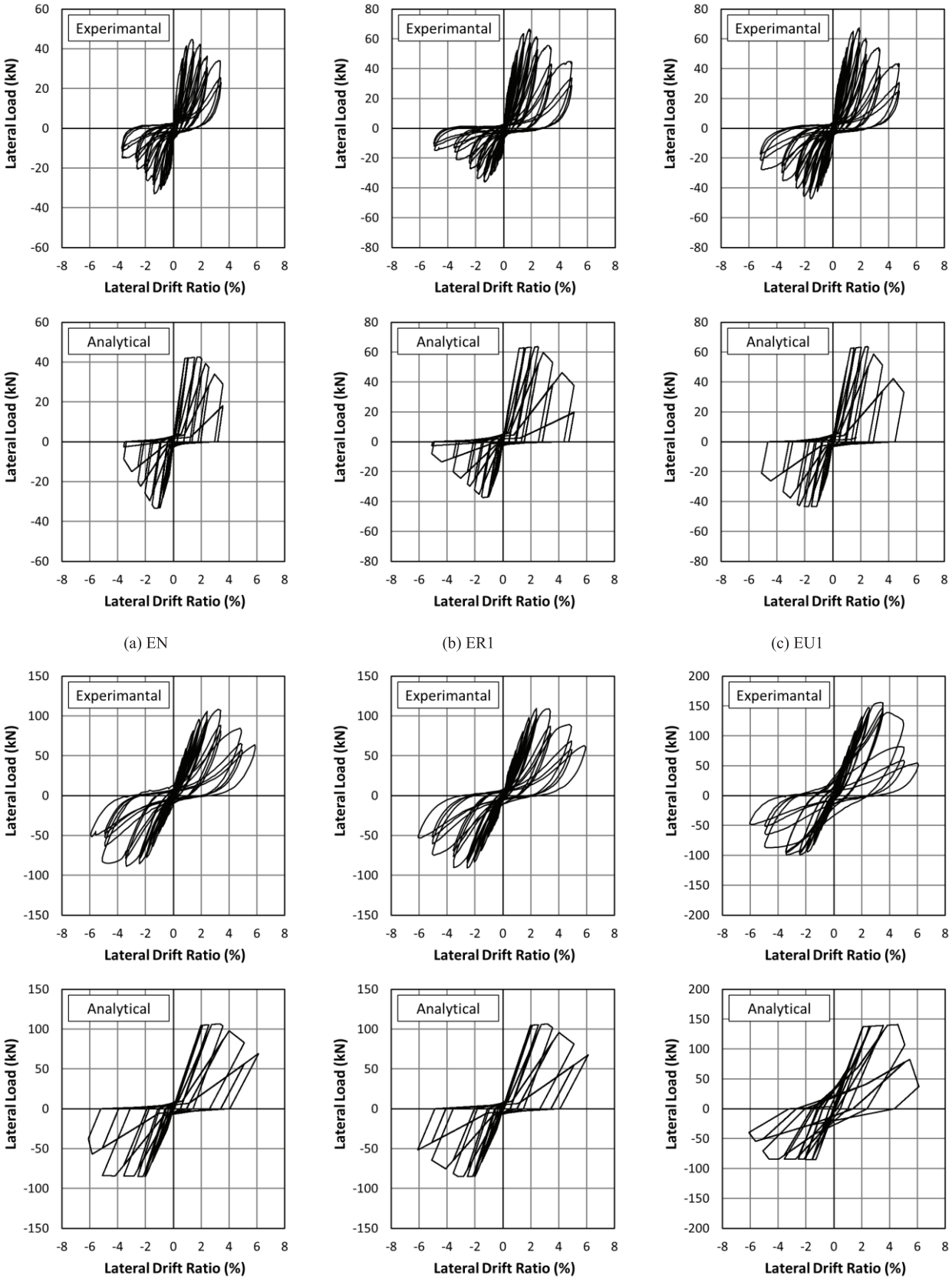

(a) EN (b) ER1 (c) EU1

(d) ER2 (e) EU2 (f) EU2C

Figure 7. Comparison of experimental and analytical hystereses for external joints

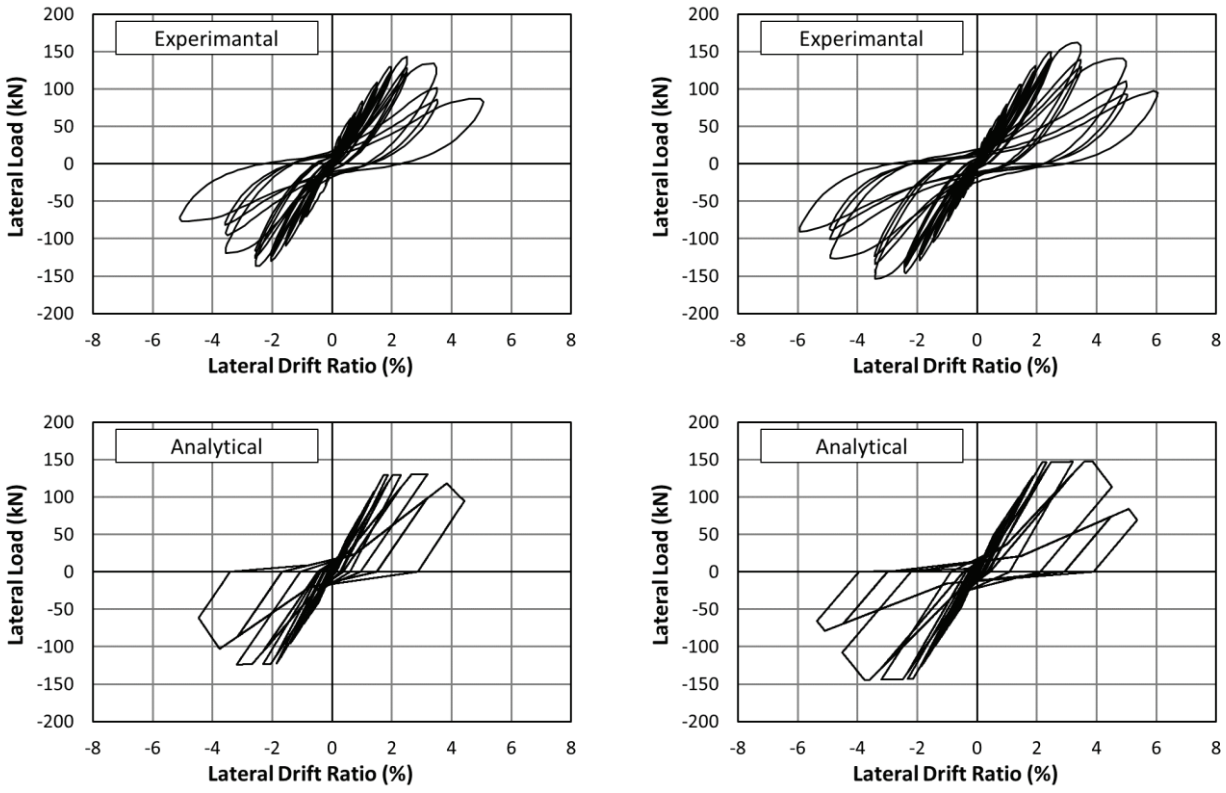

(a) IN (b) IR

Figure 8. Comparison of experimental and analytical hystereses for internal joints

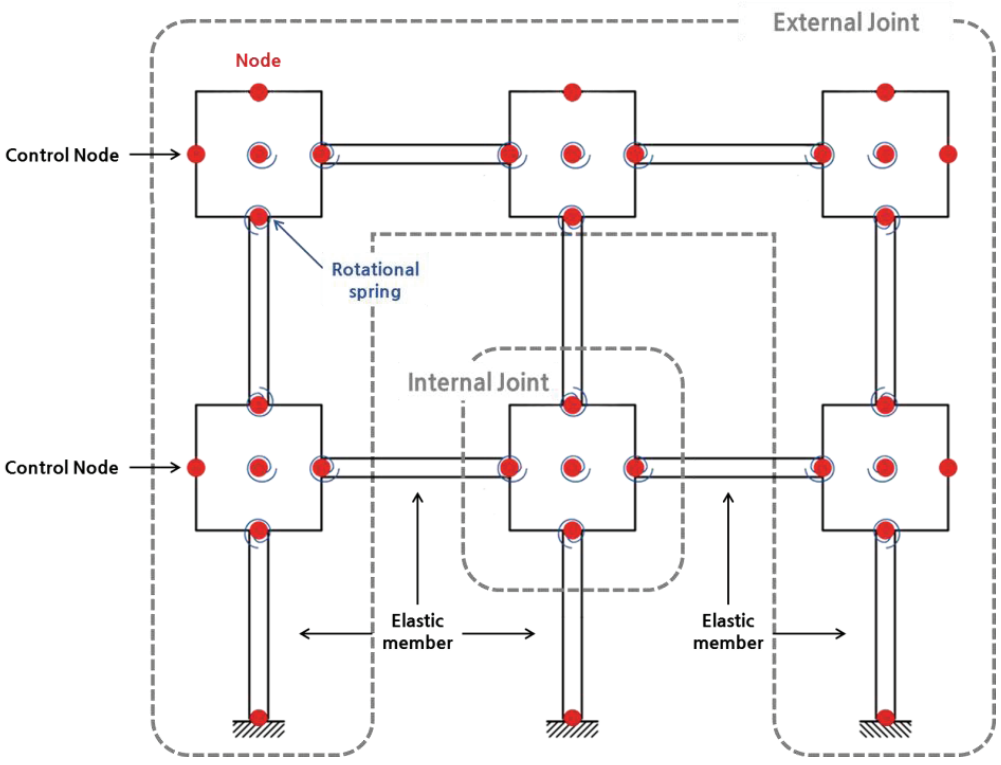

Figure 9. Schematic drawing of analytical model for two-story two-span frame specimens

5. COMPARISON OF CYCLIC BEHAVIORS OF TWO-STORY TWO-SPAN FRAMES FROM ANALYTICAL MODELS AND EXPERIMENTS

5.1. Analytical modeling of two-story two-span frames

For analytical modeling of two-story two-span frames, element models for beams, columns, and beam-column joints must be determined. However, each is a part of internal or external beam-column joint elements as shown in Figure 9. Therefore, the analytical model of two-story two-span frames can be set by a combination of internal and external beam-column joint elements. The methodology of modeling each internal or external joint element has been described above. The way to determine strength and deformation capability and cyclic deterioration modes are kept same as described in the previous section and in Kim et al. (2017) as well except some changes. For flexural plastic hinges in columns, the parameters, *rDisp* and *fFoce*, are changed to be 0.15 and 0.2, respectively, based on the hysteretic curves of the specimens. Flexural plastic hinges are assigned at both ends of beams in A1F and A2F while they are not in IMF since beams behave elastically in IMF. These changes can be attributed to the natural difference between element and system tests. Furthermore, a part of slab is added in frame specimens, but no slab exists in beam-column joint specimens. Consequently, some parameters are adjusted to match analytical results with experimental results of frame specimens while most parameters are kept same as beam-column joint specimens.

5.2. Comparison of cyclic behaviors from analytical models and experiments

Cyclic behaviors of two-story two-span frames from analytical models and experiments are shown in Figure 10. As can be noticed in the figures, the hysteretic curves of IMF from analyses simulate those from experiments pretty well. The hysteretic curves of A1F and A2F from analyses also do it well only before maximum drift, but cannot well simulate hysteresis after reaching maximum strength or drift. As can be seen in the figures, strength drops as cycles are repeated at the same drift level. In addition, strength never recover the strength before strength drops when the very next cycle increases drift level because the previous drift level is the maximum. This deficiency results from the same reason as in columns and beam-column joints. The energy part of the damage index is not incorporated in the analytical models. Even though the deficiency exists after reaching the maximum drift, the hysteretic curves well simulate those from experiments, especially pinching behavior, before reaching the maximum drift. Therefore, if nonlinear dynamic analyses are conducted by using the proposed model, the ultimate state, which can be called dynamic instability, must

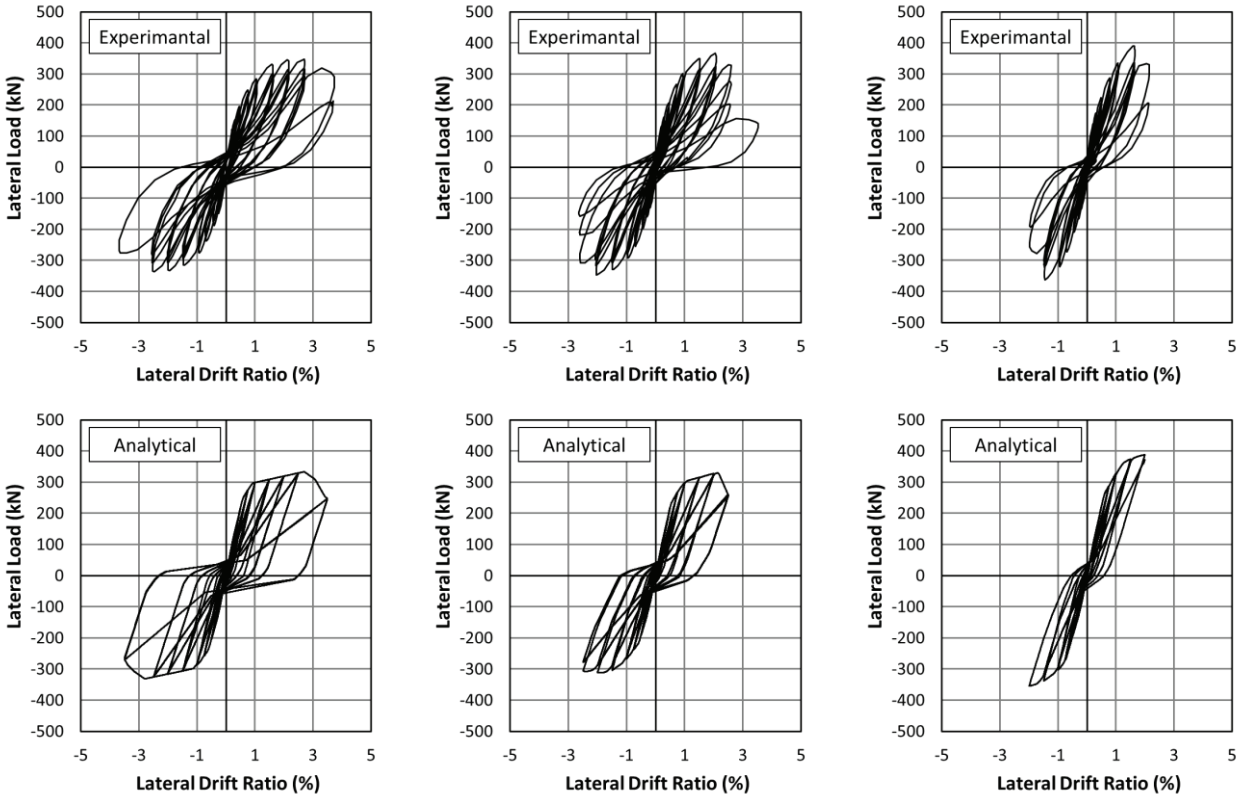

(a) IMF (b) A1F (c) A2F

Figure 9. Schematic drawing of analytical model for two-story two-span frame specimens

be checked indirectly. In other words, the ultimate state can be checked after nonlinear dynamic analyses are finished. This method is a way suggested in FEMA P695 (2009).

6. CONCLUSIONS

A nonlinear analytical model has been proposed for two-span two-story reinforced concrete frames with relaxed section details. Since the frame is composed of beams, columns, and external or internal beam-column joints, analytical modeling for each part is studied and appropriate models are proposed. The conclusions of this study are as follows.

1) The proposed model is developed to be feasible for earthquake engineering where a large number of nonlinear dynamic analyses must be required. Therefore, the analysis had better run not too long and post processing had better not be difficult to handle. In order to satisfy these conditions, all of the nonlinear behaviors are modeled to be concentrated on flexural plastic hinges at the end of beams and columns, and the center of beam-column joints. As the result, the proposed model is simple and light, which makes it easy to developing a nonlinear model of the entire frame and helps to save time to operate nonlinear analyses.
2) The deformation capability and hysteretic rules for beam-column joints and two-story two-span frames are determined based on experimental results. No theoretical approach is incorporated in developing those parameters. Some features such as strength drop in repeated cycles at the same drift or at increasing drift are not included in the model. Nevertheless, the proposed model can simulate the experimental results well enough for nonlinear analyses in earthquake engineering. Therefore, one can get an adequate model for reinforced concrete frames with relaxed section details by using the modeling approach proposed in this study.

The deficiency of the model may be compensated by conducting a large number of analyses and applying reliability and statistics to the analysis results.

REFERENCES

Altoonatash, A. (2004) Simulation and Damage Models for Performance Assessment of Reinforced Concrete Beam-Column Joints. Dissertation, Stanford University, Stanford

ASCE/SEI 41-13. (2013) Seismic Evaluation and Retrofit of Existing Buildings. Virginia, USA: American Society of Civil Engineers, p.555.

Federal Emergency Management Agency. (2009) Quantification of Building Seismic Performance Factors, FEMA P695. Prepared by the Applied Technology Council for the Federal Emergency Management Agency, Washington D. C.

Haselton, C.B., Liel, A.B., Taylor Lange, S., and Deierlein, G.G. (2008) Beam-Column Element Model Calibrated for Predicting Flexural Response Leading to Global Collapse of RC Frame Buildings, PEER Report 2007/03, Pacific Earthquake Engineering Research Center, University of California, Berkeley, California.

Ibarra L.F., & Medina R.A., and Krawinkler, H. (2005) Hysteretic Models that Incorporate Strength and Stiffness Deterioration. Earthquake Engineering and Structural Dynamics, 34(12):1489-1511.

KBC2016. (2016) Korean Building Code-Structural. Seoul, Korea: Architectural Institute of Korea.

Kim, C., Eom, T., Park, H., Kim, T. (2015b) Seismic Performance of RC Columns with Lap Splices at Plastic Hinge Region. Journal of the Architectural Institute of Korea Structure & Construction, 31(12):23-33.

Kim, C., Eom, T., Park, H., Kim, T. (2016b) Seismic Performance of Lightly Reinforced Concrete Beam-Column Connections for Low-Rise Buildings. Journal of the Architectural Institute of Korea Structure & Construction, 32(3):19-32.

Kim, C., Park, H., Eom, T., Kim, T. (2015a) Effects of Tie Details on Seismic Performance of RC Columns Subjected to Low Compression Loads. Journal of the Earthquake Engineering Society of Korea, 19(4):195-205.

Kim, C., Park, H., Kim, T., Eon, T. (2016a) Effects of Lap Splice Details on Seismic Performance of RC Columns. Journal of the Earthquake Engineering Society of Korea, 20(6):351-360.

Kim, T., Chu, Y., Park, H. (2017) Analytical Modeling for Reinforced Concrete Columns with Relaxed Section Details. Architectural Research, 19(3):79-87.

Lignos, D. (2008) Sidesway Collapse of Deteriorating Structural Systems under Seismic Excitation. Ph.D. Thesis, Department of Civil and Environmental Engineering, Stanford University, Stanford, CA, USA.

Lignos, D.G., & Krawinkler, H. (2012) Development and Utilization of Structural Component Databases for Performance-Based Earthquake Engineering. Journal of Structural Engineering, 139(8):1382-1394.

Lowes, L.N., Mitra N., and Altoontash A. (2003b) A Beam-Column Joint Model for Simulating the Earthquake Response of Reinforced Concrete Frames. Pacific Earthquake Engineering Research Center report, p.66.

Medina, R., & Krawinkler, H. (2003) Seismic Demands for Nondeteriorating Frame Structures and Their Dependence on Ground Motions. Report No. TR 144, John A. Blume Earthquake Engineering Center, Department of Civil Engineering, Stanford University, Stanford, California, and PEER Report 2003/15, Pacific Earthquake Engineering Research Center, University of California, Berkeley, California.

OpenSees. (2006) Open System for Earthquake Engineering Simulation. [online] Available at: http://opensees.berkeley.edu.

Pacific Earthquake Engineering Research Center. (2003) Structural Performance Database, University of California, Berkeley, Available from: http://nisee.berkeley.edu/spd/ and http://maximus.ce.washington.edu/~peera1/ (March 10, 2005).

Park, H. (2017) Two-story Two-span Frame Scaled Test, SPEC-R201711001, Structural Performance Enhancement Research Center, Seoul National University.
Park, Y.J. and Ang, A.H.-S. (1985) Mechanistic Seismic Damage Model for Reinforced Concrete, Journal of Structural Engineering. 111(4), 722-739.
PEER/ATC-72-1. (2010) Modeling and Acceptance Criteria for Seismic Design and Analysis of Tall Buildings, Pacific Earthquake Engineering Research Center, PEER Report 2010/111, University of California, Berkeley, California.
Stevens N.J., Uzumeri, S.M. and Collins, M.P. (1991) Reinforced-Concrete Subjected to Reversed-Cyclic Shear – Experiments and Constitutive Model. ACI Structural Journal, 88(2), 135-146.
(Received Oct. 12, 2017/Revised Jun. 5, 2018/Accepted Jun. 21, 2018)